Massive MIMO based underlay networks with power control

S. Kusaladharma and C. Tellambura, *Fellow*, *IEEE*
Department of Electrical and Computer Engineering
University of Alberta, Edmonton, Alberta T6G 2V4, Canada
Email: kusaladh@ualberta.ca and chintha@ece.ualberta.ca

Abstract—While massive MIMO based underlay cognitive radio (CR) networks are a promising concept in the next generation of wireless networks to increase spectral efficiency, reusing the same pilot sequences in both networks cause pilot contamination leading to residual interference. Thus, this paper investigates the affects of pilot contamination on a random CR network underlaid upon a random primary network where both networks employ path loss inversion based power control. A Matern cluster process is considered for the underlay system, while homogeneous Poisson point processes are considered for the primary transmitters and receivers. We derive the moment generating function of the normalized aggregate interference at an underlay receiver, its first two moments, and the outage probability. Finally, it is shown that the underlay cluster radius, ensured received power levels through power control and the different node densities have a significant effect on the outage of an underlay receiver.

I. INTRODUCTION

Spectrum limitations and interference among users sharing the same spectrum are major bottlenecks for the future growth of wireless communication systems. Underlay cognitive radio (CR) networks allow simultaneous spectrum access for both primary and secondary users to increase spectral efficiency [1], and have been proposed as a candidate technology for future fifth generation (5G) wireless systems [2]–[4]. Underlay CR techniques are widely applied for device-to-device communications, sensor networks, and cognitive femtocells in heterogeneous networks. While traditional CR techniques share spectrum on an interference free basis, underlay networks accomplish this on an interference tolerant basis which boosts spectral efficiency [2]. However, simultaneous spectrum access may significantly decrease user performance due to interference. Thus, transmit power control techniques and interference cancellation schemes are essential for primary and secondary networks to coexist with each other [2].

On another note, massive multiple input multiple output (MIMO) systems, which enable an extremely large number of antennas at the transmitter are also deemed an exciting prospect for future 5G networks [5]. Massive MIMO systems offer simultaneous service to a large number of users, increased spectral and energy efficiency over conventional MIMO and have the added advantage of negating the effects of small scale fading and noise [2]. However, one drawback of serving a large number of users simultaneously is the need to obtain channel state information (CSI) for all channels which needs periodic pilot transmissions. In addition to using a portion of the spectrum, pilot contamination is a major issue which limit potential spectral and throughput gains in massive MIMO systems [5].

The combination of CR networks and massive MIMO systems offers exciting possibilities for increased spectral efficiency coupled with potential interference cancellation. However, along with these come challenges related to pilot contamination. Primary and secondary user devices can encompass transmit power control to limit interference and increase their energy efficiency which complicates matters. Moreover, modern cell deployment is not fixed, and spatial randomness comes into the fray. Thus, it is vital to characterize the user performance considering all these factors to understand the potentials and limits of underlaid CR networks using massive MIMO.

A. Prior Research

Massive MIMO based underlaid CR networks is an emerging research area. The interplay between massive MIMO and device-to-device networks is studied in [6] under perfect and imperfect CSI at the receivers while [7] studies trade-offs between average sum rate and energy efficiency for device to device networks employing massive MIMO. Other works consider interference issues in randomly deployed base stations employing massive MIMO. For example, [8] derives closed-form expressions for the base station density bounded by the maximum outage probability under a stochastic geometry based model, while [9] obtains expressions for the signal to interference ratio for both uplink and downlink under orthogonal and non-orthogonal pilot sequences. Furthermore, the uplink of a wireless network using linear minimum mean square error spatial processing is analyzed in [10]. Moreover, [11] analyzes the coverage probability and area spectral efficiency for a heterogeneous network incorporating a massive MIMO base station.

B. Motivation and Contribution

Although substantive research is beginning to emerge, previous work on interference characterization in random wireless networks with massive MIMO enabled base stations do not consider power control for neither data or pilot signals. While being more analytically tractable, this assumption may not be the case in practice. Furthermore, other works only consider a single cell with one massive MIMO enabled base station while others only consider a single network of base stations. However, in an underlaid CR network, the differentiation of primary and secondary networks is important.

To this end, we will model the primary base stations and receivers as two homogeneous Poisson point processes (PPPs)

and the underlay network as a Matern cluster process with the underlay base stations representing cluster heads distributed as a homogeneous PPP. Log distance path loss and Rayleigh fading are assumed for channels, and a path loss inversion based power controlling scheme is considered for all signals. Primary receivers associate with their closest base station while underlay receivers associate with their cluster head. Furthermore, both primary and underlay base stations are assumed to employ massive MIMO, and CSI is obtained via uplink pilots. Finally, the moment generating function (MGF), mean and variance of the normalized aggregate interference is calculated along with the outage probability for a typical underlay receiver within a given cluster.

Notations: $\Gamma(x, a) = \int_a^\infty t^{x-1} e^{-t} dt$ and $\Gamma(x) = \Gamma(x, 0)$ [12]. $\Pr[A]$ is the probability of event A, $f_X(\cdot)$ is the probability density function (PDF), $M_X(\cdot)$ is the MGF, and $E_X[\cdot]$ denotes the expectation over random variable X.

II. SYSTEM MODEL

A. Spatial Model

This section describes the spatial distribution of primary and underlay nodes.

1) Primary Network: The primary network consists of primary transmitters and receivers. A single class of primary transmitters (base stations) distributed randomly in the $\mathbb{R}^2$ plane is considered. Although primary node locations are not purely random, it has been shown that a PPP based model provides a reasonably accurate approximation to planned node placements while providing analytical tractability [13]. The PPP model has thus been extensively used in literature to model base station locations [14]–[17]. Let the primary transmitters be distributed as a stationary homogeneous PPP $\Phi_{p,t}$ with intensity $\lambda_{p,t}$. Due to the homogeneity of $\Phi_{p,t}$, $\lambda_{p,t}$ is a constant over all $\mathbb{R}^2$. The number of primary transmitters within any closed area $\mathcal{B}$ follows the Poisson distribution with [18]

$$\Pr[N(\mathcal{B}) = n] = \frac{(\lambda_{p,t} \mathcal{B})^n}{n!} e^{-\lambda_{p,t} \mathcal{B}}. \tag{1}$$

The primary receivers are also modelled according to a homogeneous PPP. Let this process be $\Phi_{p,r}$ having an intensity $\lambda_{p,r}$. $\Phi_{p,r}$ and $\Phi_{p,t}$ are considered to be independent, stationary, and motion invariant.

2) Underlay Network: The underlay network is assumed to consist of multiple node clusters centered around underlay base stations [19]. A wireless local area network or a nano/pico cell base station would be examples of such a scenario where clustering would occur [20]. Therefore, we will model the underlay network as a Matern cluster process [19]–[21]. The cluster centres correspond to the base stations, and follow a homogeneous PPP ($\Phi_{u,t}$) with density $\lambda_{u,t}$. The daughter processes denoted as $\Phi_{u,r}$ correspond to the receivers, and are uniformly distributed within their respective clusters with density $\lambda_{u,r}$. Furthermore, the different daughter processes are assumed to be independent and stationary, and the clusters are assumed to have a diameter of d_l.

B. Signal Model

Universal frequency reuse is assumed within the primary network, and the active underlay transmitters utilizes that same frequency. Both underlay and primary receivers are assumed to be single antenna devices while primary transmitters and underlay transmitters have M and N antennas respectively. M and N have the relationship $M = \kappa N$. M and N are assumed to be large enough to serve all associated users. A time division duplex (TDD) scheme is assumed for both primary and underlay networks.

1) Channel: Both primary and underlay networks utilize pilot signalling in the uplink channel in order to obtain CSI for the downlink. The pilots are of length L, and are orthogonal with each other. If $b_a, b_b \in \mathbb{C}^{L \times 1}$ are pilot sequences, $b_a^* b_b = 0$ whenever $a \neq b$. We assume that there exist q orthogonal pilots, and that the same set of q pilots is used in all Voronoi cells by the base stations. Furthermore, this same set of pilots is used by the underlay network in all its clusters. If different pilots are used by the underlay system, our analysis would represent a worst-case scenario.

All channels are assumed to undergo Rayleigh fading and power-law path loss. Moreover, the fading between all links is assumed to be uncorrelated. Under Rayleigh fading, the channel power gain $|h|^2$ is an exponential random variable with PDF $f_{|h|^2}(x) = e^{-x}$, while with power-law path loss, the received power at a distance r from the transmitter can be written as $P = P_T r^{-\alpha}$ [22], where α is the path loss exponent and P_T is the transmit power.

2) Association and power control: In the primary network, each receiver associates with its closest transmitter, which is equivalent to associating with the transmitter providing the best average received power. In other words, the primary transmitters form Voronoi cells, and associate with receivers within its cell. For the underlay network, each receiver within a single cluster associates with its parent node.

Both underlay and primary networks employ path loss inversion based power control to ensure a fixed average power at receivers. If P_u, P_p, $P_{p,u}$ and $P_{p,p}$ are respectively the ensured power levels of underlay transmissions, primary transmissions, underlay pilots, and primary pilots, the transmit power P_T is written as $P_T = P_k r^\alpha$, where r is the transmitter-receiver distance and $P_k \in \{P_u, P_p, P_{p,u}, P_{p,p}\}$. Moreover, power scaling is employed by the primary and underlay base stations where the downlink transmitted signal is scaled by $\frac{1}{\sqrt{M}}$ and $\frac{1}{\sqrt{N}}$ respectively to compensate for the number of transmitter antennas

III. CHANNEL ESTIMATION

For both primary and underlay base stations to estimate the downlink channel, an intitial uplink training phase occurs where the primary and underlay receivers transmit pilot sequences to their serving base stations. We assume that the training phase for all base stations occur at the same time instance regardless of whether they are part of the primary or underlay network. This assumption leads to the worst case

scenario when similar pilot sequences are contaminated with each other. Furthermore, we assume a slow fading channel where the channel gains do not change between the training phase and the downlink data transmission phase.

A. Primary system

We now look at the set of pilot signals using the a-th pilot sequence arriving at a primary base station. However, only a subsection of the primary and underlay base stations will use the a-th pilot sequence. As such, we will represent the primary and underlay base stations utilizing the a-th pilot sequence by $\bar{\Phi}_{p,t}$ and $\bar{\Phi}_{u,t}$ respectively. Let $\phi_{pr,la}$ and $\phi_{ur,wa}$ respectively be the primary receiver using the a-th pilot sequence connected to $\bar{\phi}_{p,t,l}$ and the underlay receiver using the a-th pilot sequence connected to $\bar{\phi}_{u,t,w}$, where $\bar{\phi}_{p,t,l}$ is the l-th primary transmitter $\in \bar{\Phi}_{p,t}$ and $\bar{\phi}_{u,t,w}$ is the w-th underlay transmitter $\in \bar{\Phi}_{u,t}$.

The received signal y_k at the k-th primary base station ($\bar{\phi}_{p,t,k} \in \bar{\Phi}_{p,t}$) will be comprised of all pilot signals using different pilot sequences from all associated primary receivers and underlay receivers. However, without the loss of generality, as orthogonal pilots are used, we restrict our attention to the signals containing the a-th pilot sequence. Let $\bar{y}_{ka}$ denote the received signal corresponding to the a-th pilot sequence. Then, $\bar{y}_k$ is written as

$$\bar{y}_{ka} = \sum_{l=1}^{\infty} \mathbf{h}_{kla} r_{kla}^{\frac{-\alpha}{2}} b_a^T \sqrt{P_{p,p}} r_{la}^{\frac{\alpha}{2}} + \sum_{w=1}^{\infty} \mathbf{h}_{kwa} r_{kwa}^{\frac{-\alpha}{2}} b_a^T \sqrt{P_{p,u}} r_{wa}^{\frac{\alpha}{2}} + \mathbf{w}_k \quad (2)$$

where $\mathbf{h}_{kla}$ and r_{kla} are the channel gain and path loss between $\bar{\phi}_{p,t,k}$ and $\phi_{pr,la}$, $\mathbf{h}_{kwa}$ and r_{kwa} are the channel gain and path loss between $\bar{\phi}_{p,t,k}$ and $\phi_{ur,wa}$, r_{la} is the path loss between $\phi_{pr,la}$ and $\bar{\phi}_{p,t,l}$, r_{wa} is the path loss between $\phi_{ur,wa}$ and $\bar{\phi}_{u,t,w}$, and $\mathbf{w}_k$ is the received noise. The received signal $\bar{y}_{ka} \in \mathbb{C}^{M \times L}$, $\mathbf{w}_k \in \mathbb{C}^{M \times L}$, and $\mathbf{h}_{kla}, \mathbf{h}_{kwa} \in \mathbb{C}^{M \times 1}$.

The objective of $\bar{\phi}_{p,t,k}$ is to estimate the channel gain between it and $\phi_{pr,ka}$, where $\phi_{pr,ka} \in \Phi_{p,r}$ is the primary receiver using the a-th pilot sequence associated with $\bar{\phi}_{p,t,k}$. If this channel gain is denoted as $\mathbf{h}_{kka}$, the estimated channel gain $\hat{\mathbf{h}}_{kka}$ may be expressed as

$$\hat{\mathbf{h}}_{kka} = \frac{\bar{y}_{ka} b_a}{\sqrt{P_{p,p}}}$$

$$= \mathbf{h}_{kka} + \sum_{l=1 \backslash k}^{\infty} \mathbf{h}_{kla} r_{kla}^{\frac{-\alpha}{2}} r_{la}^{\frac{\alpha}{2}} + \sum_{w=1}^{\infty} \mathbf{h}_{kwa} r_{kwa}^{\frac{-\alpha}{2}} \sqrt{\frac{P_{p,u}}{P_{p,p}}} r_{wa}^{\frac{\alpha}{2}} + \frac{\mathbf{w}_k b_a}{\sqrt{P_{p,p}}}. \quad (3)$$

B. Underlay system

Within this subsection, we derive the estimated channel gain between the z-th underlay base station $\bar{\phi}_{u,t,z} \in \bar{\Phi}_{u,t}$ and its associated underlay receiver using the a-th pilot sequence $\phi_{ur,za}$. If $\bar{y}_{za} \in \mathbb{C}^{N \times L}$ is the received signal at $\bar{\phi}_{u,t,z}$ corresponding to the a-th pilot sequence,

$$\bar{y}_{za} = \sum_{l=1}^{\infty} \mathbf{h}_{zla} r_{zla}^{\frac{-\alpha}{2}} b_a^T \sqrt{P_{p,p}} r_{la}^{\frac{\alpha}{2}} + \sum_{w=1}^{\infty} \mathbf{h}_{zwa} r_{zwa}^{\frac{-\alpha}{2}} b_a^T \sqrt{P_{p,u}} r_{wa}^{\frac{\alpha}{2}} + \mathbf{w}_z, \quad (4)$$

where the notation is analogous to the previous subsection. The estimated channel gain $\mathbf{h}_{zza}$ is obtained in a similar way to (3) as

$$\hat{\mathbf{h}}_{zza} = \frac{\bar{y}_{za} b_a}{\sqrt{P_{p,u}}}$$

$$= \mathbf{h}_{zza} + \sum_{w=1 \backslash z}^{\infty} \mathbf{h}_{zwa} r_{zwa}^{\frac{-\alpha}{2}} r_{wa}^{\frac{\alpha}{2}} + \sum_{l=1}^{\infty} \mathbf{h}_{zla} r_{zla}^{\frac{-\alpha}{2}} \sqrt{\frac{P_{p,p}}{P_{p,u}}} r_{la}^{\frac{\alpha}{2}} + \frac{\mathbf{w}_z b_a}{\sqrt{P_{p,u}}}. \quad (5)$$

IV. DOWNLINK TRANSMISSION

A. Interference from primary transmitters

After channel estimation is performed by a primary transmitter, it will transmit the intended data symbols to their associated receivers in the downlink. We will assume that the downlink transmissions to receivers which used the a-th pilot sequence happen at the same time. In other words, the base stations operate in a synchronous manner. This assumption leads to a worst case scenario vis a vis interference due to pilot contamination.

Each base station $\bar{\phi}_{p,t,j} \in \bar{\Phi}_{p,t}$ uses a precoding scheme where the transmit symbol to $\phi_{pr,ja}$ is precoded with the estimated channel gain $\hat{\mathbf{h}}_{jja}$. This process occurs for all associated receivers, and the summation of the precoded signals are transmitted [9].

Our objective is to obtain the received signal at a typical underlay receiver utilizing the a-th pilot signal. Let $\phi_{ur,za}$ denote this node which is associated with the z-th underlay base station $\bar{\phi}_{u,t,z}$. The received interference from primary base stations at $\phi_{ur,za}$ is written as

$$Y_{za,p} = \sum_{j=1}^{\infty} \mathbf{h}_{jza}^* r_{jza}^{\frac{-\alpha}{2}} x_j, \quad (6)$$

where $\mathbf{h}_{jza}^*$ and $r_{jza}^{\frac{-\alpha}{2}}$ are the channel gain and path loss between $\bar{\phi}_{p,t,j}$ and $\phi_{ur,za}$, and x_j is the transmit symbol by $\bar{\phi}_{p,t,j}$. $\mathbf{h}_{jza}^*$ is the reciprocal of the channel gain between $\phi_{ur,za}$ and $\bar{\phi}_{p,t,j}$ because a TDD system is considered. The transmitted symbol x_j is expressed as

$$x_j = \sum_{\nu=1}^{q_j} \hat{\mathbf{h}}_{jj\nu} \sqrt{\frac{P_p}{M}} r_{jj\nu}^{\frac{\alpha}{2}} d_{j\nu}, \quad (7)$$

where $q_j (< q)$ is the number of associated primary receivers of $\bar{\phi}_{p,t,j}$, $\hat{\mathbf{h}}_{jj\nu}$ and $r_{jj\nu}$ are the estimated uplink channel and path loss between $\bar{\phi}_{p,t,j}$ and $\phi_{pr,j\nu}$, and $d_{j\nu}$ is the data symbol intended for $\phi_{pr,j\nu}$. After normalising $Y_{za,p}$ with respect to $\sqrt{M}$, the received interference from primary base stations is written as

$$\tilde{Y}_{za,p} = \lim_{M \to \infty} \frac{Y_{za,p}}{\sqrt{M}}$$

$$= \lim_{M \to \infty} \frac{1}{M} \sum_{j=1}^{\infty} \mathbf{h}_{jza}^* r_{jza}^{\frac{-\alpha}{2}} \sqrt{P_p} \sum_{\nu=1}^{q_j} r_{jj\nu}^{\frac{\alpha}{2}} d_{j\nu} \times$$

$$\left(\mathbf{h}_{jj\nu} + \sum_{l=1 \backslash j}^{\infty} \mathbf{h}_{jl\nu} r_{jl\nu}^{\frac{-\alpha}{2}} r_{l\nu}^{\frac{\alpha}{2}} + \sum_{w=1}^{\infty} \mathbf{h}_{jw\nu} r_{jw\nu}^{\frac{-\alpha}{2}} \sqrt{\frac{P_{p,u}}{P_{p,p}}} r_{w\nu}^{\frac{\alpha}{2}} + \frac{\mathbf{w}_j b_\nu}{\sqrt{P_{p,p}}} \right) \quad (8)$$

However, $\lim_{M \to \infty} \frac{\mathbf{h}_{jza}^* \mathbf{h}_{jl\nu}}{M} \to 0, \forall j, \nu, l$ because independent and identically distributed channel gains are considered for different links, and $\lim_{M \to \infty} \frac{\mathbf{h}_{jza}^* \mathbf{w}_j b_\nu}{M} \to 0, \forall j$. Furthermore, $\lim_{M \to \infty} \frac{\mathbf{h}_{jza}^* \mathbf{h}_{jw\nu}}{M} \to 1$ whenever $w = z, \nu = a$. Thus, $\tilde{Y}_{za,p}$ can be expressed as

$$Y_{za,p}^{\sim} = \sum_{j=1}^{\infty} \sqrt{\frac{P_p P_{p,u}}{P_{p,p}}} r_{jza}^{-\alpha} r_{jja}^{\frac{\alpha}{2}} r_{za}^{\frac{\alpha}{2}} d_{ja}. \tag{9}$$

B. Downlink signal from underlay transmitters

Similar to the downlink transmission from primary base stations, each underlay base station $\bar{\phi}_{u,t,i} \in \bar{\Phi}_{u,t}$ precodes its symbol to $\phi_{ur,ia}$ with the estimated channel gain $\hat{h}_{iia}$. We will assume that downlink transmissions from all underlay transmitters occur at the same time. The received signal from underlay base stations at $\phi_{ur,za}$ is thus written as

$$Y_{za,u} = \sum_{i=1}^{\infty} \mathbf{h}_{iza}^* r_{iza}^{\frac{-\alpha}{2}} x_i, \tag{10}$$

where x_i is defined by

$$x_j = \sum_{\nu=1}^{q_i} \hat{\mathbf{h}}_{ii\nu} \sqrt{\frac{P_u}{N}} r_{ii\nu}^{\frac{\alpha}{2}} d_{i\nu}. \tag{11}$$

The number of associated underlay receivers of $\bar{\phi}_{u,t,i}$ is denoted by $q_i (< q)$. After normalizing $Y_{za,u}$ with respect to $\sqrt{M}$, the signal from the underlay base stations is written as

$$\tilde{Y}_{za,u} = \lim_{M \to \infty} \frac{Y_{za,u}}{\sqrt{M}}$$
$$= \lim_{N \to \infty} \frac{1}{\sqrt{\kappa}N} \sum_{i=1}^{\infty} \mathbf{h}_{iza}^* r_{iza}^{\frac{-\alpha}{2}} \sqrt{P_u} \sum_{\nu=1}^{q_i} r_{ii\nu}^{\frac{\alpha}{2}} d_{i\nu} \times$$
$$\left(\mathbf{h}_{ii\nu} + \sum_{w=1\backslash i}^{\infty} \mathbf{h}_{iw\nu} r_{iw\nu}^{\frac{-\alpha}{2}} r_{w\nu}^{\frac{\alpha}{2}} + \sum_{l=1}^{\infty} \mathbf{h}_{il\nu} r_{il\nu}^{\frac{-\alpha}{2}} \sqrt{\frac{P_{p,p}}{P_{p,u}}} r_{l\nu}^{\frac{\alpha}{2}} + \frac{\mathbf{w}_i b_\nu}{\sqrt{P_{p,u}}} \right)$$
$$= \frac{\sqrt{P_u}}{\sqrt{\kappa}} + \sum_{i=1\backslash z}^{\infty} \frac{\sqrt{P_u}}{\sqrt{\kappa}} r_{iza}^{-\alpha} r_{iia}^{\frac{\alpha}{2}} r_{za}^{\frac{\alpha}{2}} d_{ia}. \tag{12}$$

The first term of (12) represents the desired signal to $\phi_{ur,za}$ while the second term represents the interference from underlay transmitters.

C. Interfering base station density

In the previous subsections, it was found out that the interference to $\phi_{ur,za}$ occurs from primary and underlay transmitters using the a-th pilot sequence (namely $\bar{\Phi}_{p,t}$ and $\bar{\Phi}_{u,t}$). This subsection derives the densities of these processes.

1) Density of $\bar{\Phi}_{p,t}$: Let $\bar{\lambda}_{p,t}$ be the density of $\bar{\Phi}_{p,t}$. We can approximate $\bar{\Phi}_{p,t}$ as a thinned PPP [23] where the density $\bar{\lambda}_{p,t} = \eta \lambda_{p,t}$. The factor η is the probability that a particular base station uses the a-th pilot sequence.

We will consider a typical primary base station $\phi_{p,t,k} \in \Phi_{p,t}$. The number of users associated with $\phi_{p,t,k}$ is a random variable depending on the area of its Voronoi cell (S). However, the area distribution of a Voronoi cell has no known

exact distributions. In [24] a two parameter gamma empirical approximation has been shown to fit the exact size distribution where the normalized cell size $\tilde{S} = \frac{S}{\bar{S}}$ follows

$$f_{\tilde{S}}(y) \approx \frac{\beta^\mu}{\Gamma(\mu)} y^{\mu-1} e^{-\beta y}, \tag{13}$$

where $\mu = 3.61$, $\beta = 3.57$, and $\bar{S}$ is the average size of a cell given by $\bar{S} = \frac{1}{\lambda_{p,t}}$.

Let ω_1 be the number of associated users with $\phi_{p,t,k}$. When $\omega_1 \geq q$, all the pilot sequences will be used whereas when $\omega_1 < q$ there exists a probability that the a-th pilot sequence is not used by any user associated with $\phi_{p,t,k}$. Thus, we can write η as

$$\eta = \Pr[\omega_1 \geq q] + \Pr[\omega_1 < q] \frac{E_{\omega_1 \backslash \omega_1 < q}[\omega_1]}{q}$$
$$= E_S \left[\sum_{n=q}^{\infty} \frac{(\lambda_{p,r} S)^n}{n!} e^{-\lambda_{p,r} S} + \frac{1}{q} \sum_{\omega_1=1}^{q-1} \frac{(\lambda_{p,r} S)^{\omega_1}}{\omega_1 - 1!} e^{-\lambda_{p,r} S} \right] . \tag{14}$$

Substituting $S = \tilde{S}\bar{S}$ and performing the expectation with respect to (13) we obtain

$$\eta = \frac{\beta^\mu}{\Gamma(\mu)} \sum_{n=q}^{\infty} \frac{\Gamma(\mu+n)}{n!(\beta + \frac{\lambda_{p,r}}{\lambda_{p,t}})^{\mu+n}} \left(\frac{\lambda_{p,r}}{\lambda_{p,t}} \right)^n$$
$$+ \frac{1}{q} \frac{\beta^\mu}{\Gamma(\mu)} \sum_{\omega_1=1}^{q-1} \frac{\Gamma(\mu+\omega_1)}{(\omega_1-1)!(\beta + \frac{\lambda_{p,r}}{\lambda_{p,t}})^{\mu+\omega_1}} \left(\frac{\lambda_{p,r}}{\lambda_{p,t}} \right)^{\omega_1} . \tag{15}$$

2) Density of $\bar{\Phi}_{u,t}$: Let $\bar{\lambda}_{u,t}$ be the density of $\bar{\Phi}_{u,t}$. Similar to before, $\bar{\Phi}_{u,t}$ can be obtained by applying independent thinning on $\Phi_{u,t}$. Therefore, $\bar{\lambda}_{u,t} = \theta \lambda_{u,t}$, and θ is the probability that a particular underlay base station uses the a-th pilot sequence.

Let $\phi_{u,t,z} \in \Phi_{u,t}$ be a typical active underlay transmitter. Although the cluster area of $\phi_{u,t,z}$ is fixed, the number of receivers associated with it (ω_2) is still a random variable. We can thus write θ as

$$\theta = \Pr[\omega_2 > q] + \Pr[\omega_2 < q] \frac{E_{\omega_2 \backslash \omega_2 < q}[\omega_2]}{q}$$
$$= \sum_{n=q}^{\infty} \frac{(\lambda_{u,r} \frac{\pi d_l^2}{4})^n}{n!} e^{-\lambda_{u,r} \frac{\pi d_l^2}{4}} + \frac{1}{q} \sum_{\omega_2=1}^{q-1} \frac{(\lambda_{u,r} \frac{\pi d_l^2}{4})^{\omega_2}}{\omega_2 - 1!} e^{-\lambda_{u,r} \frac{\pi d_l^2}{4}} \tag{16}$$

V. INTERFERENCE CHARACTERIZATION

We now characterize the interference at $\phi_{ur,za}$ and obtain the outage probability. The aggregate interference normalized with respect to $\sqrt{M}$ (I) can be written as $I = I_p + I_u$, where $I_p = \sum_{j=1}^{\infty} \frac{P_p P_{p,u}}{P_{p,p}} r_{jza}^{-2\alpha} r_{jja}^{\alpha} r_{za}^{\alpha}$ and $I_u = \sum_{i=1\backslash z}^{\infty} \frac{P_u}{\kappa} r_{iza}^{-2\alpha} r_{iia}^{\alpha} r_{za}^{\alpha}$. Without the loss of generality, we assume that $d_{ja}^2, d_{ia}^2 = 1$. The SIR[1] (γ) at $\phi_{ur,za}$ is written as $\gamma = \frac{P_u}{\kappa(I_p+I_u)}$, and the outage probability is expressed as

$$P_O = \Pr[\gamma < \gamma_{th}] = \Pr[I > \frac{P_u}{\kappa \gamma_{th}}], \tag{17}$$

[1]Note that SIR is equal to the SINR (signal to interference and noise ratio) because the noise power approaches zero when normalized by $\sqrt{M}$.

where γ_{th} is the threshold SIR required at an underlay receiver. In order to evaluate P_O, the distribution of I is required.

To this end, we will first evaluate the MGF of I which is defined as $M_I(s) = E[e^{-sI}]$. However, because I_p and I_u are independent, $M_I(s)$ becomes $M_I(s) = E[e^{-sI_p}]E[e^{-sI_u}] = M_{I_p}(s)M_{I_u}(s)$. Using the Campbell's theorem [23], M_{I_p} is expressed as

$$M_{I_p}(s) = e^{\left(\int_0^\infty E\left[e^{-s\frac{P_p P_{p,u}}{P_{p,p}} r_{jza}^{-2\alpha} r_{jja}^{\alpha} r_{za}^{\alpha}} - 1\right] 2\pi\bar{\lambda}_{p,t} r_{jza} dr_{jza}\right)},$$ (18)

where the expectation is with respect to r_{jja} and r_{za}. Therefore, in order to evaluate (18), the distributions of r_{jja} and r_{za} are needed. The variable r_{jja} can be interpreted as the distance from a primary base station to any associated receiver. However, the receiver can be located at any point within the Voronoi cell of $\bar{\phi}_{p,t,j}$. It has been shown in [25] that r_{jja} has the approximate PDF given by

$$f_{r_{jja}}(x) \approx 2\pi\lambda_{p,t} x e^{-\pi\lambda_{p,t}x^2}, 0 < x < \infty.$$ (19)

However, it is worth noting that (19) is not the exact PDF due to correlations and dependence induced by the structure of the Voronoi tessellation. On the contrary, r_{za} which is the distance has an exact simple PDF given by

$$f_{r_{za}}(x) = \frac{2x}{(\frac{d_l}{2})^2}, 0 < x < \frac{d_l}{2}.$$ (20)

Another complication which arises is the singularity of the path loss model when the distance is 0. As a way around this issue, we use the path loss function $g(r) = min(1, r^{-\alpha})$ [26] wherever necessary. Using (20), (19), and replacing r_{jza} with r for clarity, we can simplify (18) as

$$M_{I_p}(s) = e^{\left(\int_0^\infty E_{r_{jja}, r_{za}}\left[\sum_{v=1}^{\infty} \frac{\left(-s\frac{P_p P_{p,u}}{P_{p,p}} r^{-2\alpha} r_{jja}^{\alpha} r_{za}^{\alpha}\right)^v}{v!}\right] 2\pi\bar{\lambda}_{pt} r dr\right)}$$

$$= e^{\left(\sum_{v=1}^{\infty} \frac{\pi\bar{\lambda}_{pt}}{v!}\left(\frac{-sP_p P_{p,u}}{P_{p,p}}\right)^v \left(\frac{\alpha v d_l^{\alpha v} \Gamma(\frac{\alpha v}{2}+1)}{(\alpha v-1)2^{\alpha v-1}(\alpha v+2)(\pi\lambda_{p,t})^{\frac{\alpha v}{2}}}\right)\right)}$$ (21)

From (21), it is possible to obtain the first and second order statistics of I_p as $E[I_p] = \frac{\eta P_p P_{p,u} \alpha d_l^{\alpha} \Gamma(\frac{\alpha}{2}+1)}{P_{p,p}(\alpha-1)2^{\alpha-1}(\alpha+2)(\pi\lambda_{p,t})^{\frac{\alpha}{2}-1}}$ and $Var[I_p] = \frac{\eta(P_p P_{p,u})^2 \alpha d_l^{2\alpha} \Gamma(\alpha+1)}{P_{p,p}^2(2\alpha-1)2^{2\alpha-1}(\alpha+1)(\pi\lambda_{p,t})^{\alpha-1}}$.

We now focus our attention I_u. Using the Slivnyak's theorem [9], [26], the interfering underlay base stations $(\bar{\Phi}_{u,t}\backslash z)$ can be taken as forming a homogeneous PPP. Therefore, using Campbell's theorem [23], $M_{I_u}(s)$ is written as

$$M_{I_u}(s) = e^{\left(\int_0^\infty E\left[e^{-s\frac{P_u}{\kappa} r_{iza}^{-2\alpha} r_{iia}^{\alpha} r_{za}^{\alpha}} - 1\right] 2\pi\bar{\lambda}_{u,t} r_{iza} dr_{iza}\right)},$$ (22)

where the expectation is with respect to r_{iia} and r_{za}. However, r_{iia} follows the distribution of of (20). Therefore, we can simplify (22) as

$$M_{I_u}(s) = e^{\left(\sum_{v=1}^{\infty} \frac{\pi\bar{\lambda}_{u,t}\alpha v}{v!(\alpha v-1)}\left(\frac{-sP_u}{\kappa}\right)^v \left(\frac{d_l^{\alpha v}}{2^{\alpha v-1}(\alpha v+2)}\right)^2\right)}.$$ (23)

The expectation and variance of I_u are obtained from the moments of (23) as $E[I_u] = \frac{\pi\bar{\lambda}_{u,t}\alpha P_u d_l^{2\alpha}}{\kappa(\alpha-1)(2^{\alpha-1}(\alpha+2))^2}$ and $Var[I_u] = \frac{2\pi\bar{\lambda}_{u,t}\alpha P_u^2 d_l^{4\alpha}}{\kappa^2(2\alpha-1)(2^{2\alpha}(\alpha+1))^2}$.

Now, in order to evaluate (17), I will be approximated as a gamma distribution using first and second order moment matching [27]. The resulting gamma distribution has shape and scale parameters of $\frac{(E[I_u]+E[I_p])^2}{Var[I_u]+Var[I_p]}$ and $\frac{Var[I_u]+Var[I_p]}{E[I_u]+E[I_p]}$ respectively. The outage probability of an underlay receiver is finally expressed as

$$P_O = 1 - \frac{1}{\Gamma\left(\frac{(E[I_u]+E[I_p])^2}{Var[I_u]+Var[I_p]}\right)}\gamma\left(\frac{(E[I_u]+E[I_p])^2}{Var[I_u]+Var[I_p]}, \frac{\frac{P_u}{\kappa\gamma_{th}}}{\frac{Var[I_u]+Var[I_p]}{E[I_u]+E[I_p]}}\right).$$ (24)

VI. NUMERICAL RESULTS

This provides numerical results on the outage probability of an underlay receiver with respect to different system parameters. We will use parameter values $P_{p,p} = -80\,\text{dBm}$, $P_{p,u} = -80\,\text{dBm}$, $P_u = -70\,\text{dBm}$, $q = 64$, $\gamma_{th} = 1$, and $\kappa = 1$.

Fig. 1 plots the variation of the outage probability P_O with respect to the path loss exponent α. As α increases, P_O reduces for all values of P_p and d_l. However, the rate of decline varies significantly with α. Moreover, while having a higher outage probability when other parameter values remain the same, a higher d_l also provides a greater outage variation when P_p is varied.

In Fig. 2, the outage probability is plotted with respect to the primary receiver density $\lambda_{p,r}$. From the plot, it is apparent that a complex relationship exists where there is no clear trend. However, when $\lambda_{u,t}$ and $\lambda_{p,t}$ are increased, the outage increases sharply when $\lambda_{p,r}$ is increased beyond 10^{-2}. Although a comparative an increase in $\lambda_{p,t}$ affects the outage more when $\lambda_{p,r} > 10^{-4}$, for lower $\lambda_{p,r}$, an increase in $\lambda_{u,t}$ has a greater effect on the outage. Moreover, when all other parameters remain the same, changing $\lambda_{u,r}$ has a negligible effect on the outage.

VII. CONCLUSION

This paper investigated the performance of an underlay receiver when both primary and underlay networks employ massive MIMO at their base stations, and use path loss inversion based power control. The underlay network was modeled as a Matern cluster process with the cluster centres representing base stations while the primary transmitters and receivers were modelled as homogeneous PPPs in $\mathbb{R}^2$, and all processes were assumed to be independent and stationary. The interference at an underlay receiver resulting from pilot contamination was characterized using the MGF of the normalized interference and the outage. It was observed that while an increased path loss exponent reduced the outage, the rate of decrease varied with threshold power levels and system parameters, and that transmitter densities of both networks significantly affected the outage characteristics.
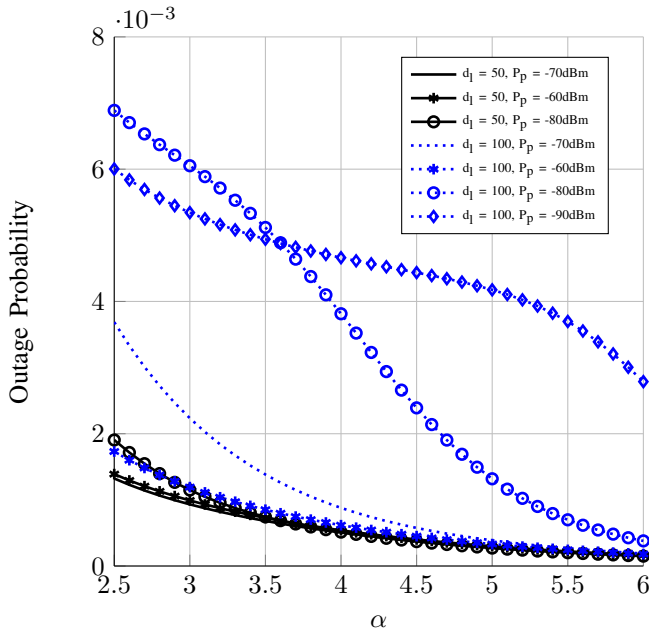
Fig. 1: Outage probability vs. the path loss exponent (α) for different values of d_l and P_p. $\lambda_{p,t} = 10^{-4}$, $\lambda_{u,t} = 10^{-4}$, $\lambda_{p,r} = 10^{-2}$, $\lambda_{u,r} = 10^{-2}$.
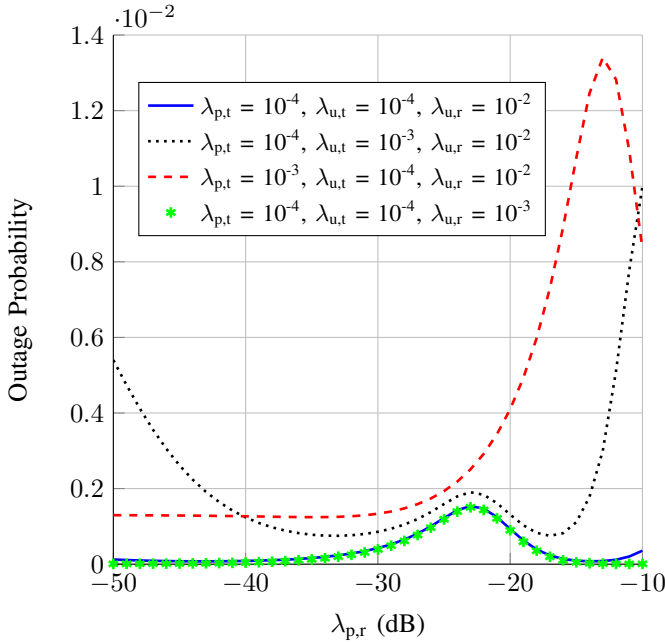

Fig. 2: Outage probability vs. the primary receiver density ($\lambda_{p,r}$) under different values of $\lambda_{p,t}$, $\lambda_{u,t}$, and $\lambda_{u,r}$. $\alpha = 3$, $P_p = -70\,\mathrm{dBm}$, $d_l = 50$.

REFERENCES

[1] S. Srinivasa and S. Jafar, "Cognitive radios for dynamic spectrum access - the throughput potential of cognitive radio: A theoretical perspective," *IEEE Commun. Mag.*, vol. 45, no. 5, pp. 73–79, May 2007.

[2] C.-X. Wang, F. Haider, X. Gao, X.-H. You, Y. Yang, D. Yuan, H. Aggoune, H. Haas, S. Fletcher, and E. Hepsaydir, "Cellular architecture and key technologies for 5g wireless communication networks," *IEEE Commun. Magazine*, vol. 52, no. 2, pp. 122–130, February 2014.

[3] A. Gupta and R. Jha, "A survey of 5g network: Architecture and emerging technologies," *IEEE Access*, vol. 3, pp. 1206–1232, 2015.

[4] X. Hong, J. Wang, C.-X. Wang, and J. Shi, "Cognitive radio in 5g: a perspective on energy-spectral efficiency trade-off," *IEEE Commun. Magazine*, vol. 52, no. 7, pp. 46–53, July 2014.

[5] V. Jungnickel, K. Manolakis, W. Zirwas, B. Panzner, V. Braun, M. Lossow, M. Sternad, R. Apelfro?jd, and T. Svensson, "The role of small cells, coordinated multipoint, and massive mimo in 5g," *Communications Magazine, IEEE*, vol. 52, no. 5, pp. 44–51, May 2014.

[6] X. Lin, R. Heath, and J. Andrews, "The interplay between massive mimo and underlaid d2d networking," *IEEE Trans. Wireless Commun.*, vol. 14, no. 6, pp. 3337–3351, June 2015.

[7] S. Shalmashi, E. Bjornson, M. Kountouris, K. W. Sung, and M. Debbah, "Energy efficiency and sum rate when massive mimo meets device-to-device communication," in *Proc. IEEE ICCW*, June 2015, pp. 627–632.

[8] X. Zou, G. Cui, M. Tang, and W. Wang, "Base station density bounded by maximum outage probability in massive mimo system," in *Proc. IEEE VTC*, May 2015, pp. 1–5.

[9] P. Madhusudhanan, X. Li, Y. Liu, and T. Brown, "Stochastic geometric modeling and interference analysis for massive mimo systems," in *Proc. IEEE WiOpt*, May 2013, pp. 15–22.

[10] S. Govindasamy, "Uplink performance of large optimum-combining antenna arrays in poisson-cell networks," in *Proc. IEEE ICC*, June 2014, pp. 2158–2164.

[11] M. Kountouris and N. Pappas, "Hetnets and massive mimo: Modeling, potential gains, and performance analysis," in *Proc. IEEE APWC*, Sept 2013, pp. 1319–1322.

[12] I. Gradshteyn and I. Ryzhik, *Table of integrals, Series, and Products*, 7th ed. Academic Press, 2007.

[13] H. Dhillon, R. Ganti, F. Baccelli, and J. Andrews, "Modeling and analysis of k-tier downlink heterogeneous cellular networks," *IEEE J. Sel. Areas Commun.*, vol. 30, no. 3, pp. 550–560, April 2012.

[14] Z. Chen, C.-X. Wang, X. Hong, J. Thompson, S. Vorobyov, X. Ge, H. Xiao, and F. Zhao, "Aggregate interference modeling in cognitive radio networks with power and contention control," *IEEE Trans. Commun.*, vol. 60, no. 2, pp. 456–468, Feb. 2012.

[15] A. Rabbachin, T. Q. S. Quek, H. Shin, and M. Z. Win, "Cognitive network interference," *IEEE J. Sel. Areas Commun.*, vol. 29, no. 2, pp. 480–493, Feb. 2011.

[16] S.-R. Cho and W. Choi, "Coverage and load balancing in heterogeneous cellular networks with minimum cell separation," *IEEE Trans. Mobile Computing*, vol. 13, no. 9, pp. 1955–1966, Sept 2014.

[17] L. Vijayandran, P. Dharmawansa, T. Ekman, and C. Tellambura, "Analysis of aggregate interference and primary system performance in finite area cognitive radio networks," *IEEE Trans. Commun.*, vol. PP, no. 99, pp. 1–12, 2012.

[18] A. Baddeley, I. Barany, R. Schneider, and W. Weil, *Spatial Point Processes and their Applications*. Springer, 2007.

[19] Y. Liu, C. Yin, J. Gao, and X. Sun, "Transmission capacity for overlaid wireless networks: A homogeneous primary network versus an inhomogeneous secondary network," in *Proc. IEEE ICCCAS*, vol. 1, Nov 2013, pp. 154–158.

[20] Y. Zhou, Z. Zhao, Q. Ying, R. Li, X. Zhou, and H. Zhang, "Two-tier spatial modeling of base stations in cellular networks," in *Proc. IEEE PIMRC*, Sept 2014, pp. 1570–1574.

[21] N. Deng, W. Zhou, and M. Haenggi, "Heterogeneous cellular network models with dependence," *IEEE J. Sel. Areas Commun.*, vol. 33, no. 10, pp. 2167–2181, Oct 2015.

[22] A. Goldsmith, *Wireless Communications*. Cambridge University Press, 2005.

[23] J. F. Kingman, *Poisson Processes*. Oxford University Press, 1993.

[24] J. Ferenc and Z. Neda, "On the size distribution of poisson voronoi cells," *Phisica A: Statistical Mechanics and its Applications*, vol. 385, no. 2, pp. 518–526, Nov 2007.

[25] T. Novlan, H. Dhillon, and J. Andrews, "Analytical modeling of uplink cellular networks," *IEEE Trans. Wireless Commun.*, vol. 12, no. 6, pp. 2669–2679, June 2013.

[26] M. Haenggi, *Stochastic Geometry for Wireless Networks*. Cambridge University Press, 2013.

[27] S. Kusaladharma and C. Tellambura, "Aggregate interference analysis for underlay cognitive radio networks," *IEEE Wireless Commun. Lett.*, vol. 1, no. 6, pp. 641–644, 2012.